JOURNAL OF MECHANICS OF CONTINUA AND MATHEMATICAL SCIENCES
www.journalimcms.org

ISSN (Online) : 2454 -7190 Vol.-19, No.-7, July (2024) pp 112-125 ISSN (Print) 0973-8975

FLOW THROUGH STEAM TURBINE CASCADE FOR ROUGHNESS ANALYSIS

Manjunath K.[1], Ajeet Singh Sikarwar[2], Naushad Ahmad Ansari[3]

[1]Mechanical Engineering Department, Delhi Technological University Delhi 110042, India

[2]Mechanical Engineering Department, Institute of Technology and Management, Gwalior 474001, India

[3]Mechanical Engineering Department, Delhi Technological University Delhi 110042, India

Email : [1]manjunath.k@dtu.ac.in, [2]ajeetsingh.sikarwar10@gmail.com, [3]naushad.nsr@gmail.com

Corresponding Author: **Naushad Ahmad Ansari**

https://doi.org/10.26782/jmcms.2024.07.00008

(Received: May 07, 2024; Revised: June 23, 2024; Accepted: July 05, 2024)

Abstract

The flow of liquids is essential to our understanding of the world. Traditionally, this is done by studying the flow of liquids using wind tunnels in the model. However, the field of computer fluid dynamics has been born over the past century. A program that can model fluid flow is CFD software. Gambit 2.4.6 created a three-dimensional geometry of four reaction blades with a square cascade and studied the secondary losses using FLUENT 6.2. The air is chosen as a working material. Air passes through the turbine cascade at a maximum input speed of 102 m/s. The cascade opens to the atmosphere when exiting. Firstly, the two surfaces of the blade cascade have been smoothed and the secondary losses analyzed. This total flow loss was compared with a roughness applied individually to the suction and pressure surfaces of 250 microns, 750 microns, and 1000 microns in thickness and examined the effect of the thickness on flow loss.

Keywords: Blade surface, Effect of roughness, End loss phenomena, Loss Coefficient, Turbine steam path.

I. Introduction

As energy savings are increasingly needed, sustainable efforts are being made worldwide to improve the efficiency of thermal power plants. Today, 80 percent of the world's electricity is produced by steam turbines. Historical divisions of loss into profile loss, end loss, and leakage loss are still widely used, but it is clear that loss

generation mechanisms are rare, but it is now widely recognized that they are independent. Final loss is the main component of internal turbine aerodynamic loss. End losses are sometimes referred to as secondary losses because they are partly generated by secondary flows generated by three-dimensional flows near the end walls. End-of-loss phenomena are mainly important for two reasons in turbo machines. First, it causes a drop in pressure in a stage and second, it makes the exit flow of a stage not uniform, which can cause a decrease in pressure losses in a downstream line. From the above-mentioned point of view, improving the efficiency of turbo machines has become a key field of research. Thus, research efforts on highly efficient turbines have improved the understanding of flow fields and the losses associated with turbine stages.

Using a k-ξ turbulence model, J. Y. Moon and K. S. Yong [X] examined how end wall fencing affected secondary flow reduction. They also justified the end wall fence's optimal placement in order to minimize losses due to secondary flow. This is because the end-wall fencing keeps the path vortex and the pressure-side horseshoe vortex from merging, which lowers overall pressure loss. Brear et al. [XI] looked into changing the leading edge geometry to lessen pressure surface separation. By expanding the force near the wall, they found that raising the sharp edge thickness at the strain surface decreases the strength of the optional stream.

Tests focus on rectangular response fountains and drive cutting edges with soft and hard surfaces by Samsher [XVII]. The 220, 100, and 50-grade emery paper roughness at the upper edge, middle harmony, and upper edge covers 33% of the surface. Attractions and resistance surfaces are gradually coated in these rough spots. Saha et al. [III] examined the violent flow through a three-layer non-axisymmetric cut tube. They found that end wall shaping brings down the pitch-wise tension slope close to the end wall, bringing down the probability of stream partition.

Singh and Kale [VIII] numerically simulated a rectilinear blade cascade with a surface roughness of up to 100 m at various turbine blade locations. It has been pointed out that the roughness affects the efficiency of the turbine blade more on the input surface than on the pressure side. When the roughness is placed on the subsequent edge of the suction surface instead of on the middle chord, the mass-average profile losses are higher and the losses are lower when the top edge is rough. Sonoda et al. [XIX] used the axis symmetrical contour method for the end wall. To minimize secondary losses in low-view high-pressure turbines. They investigated the effects of three different techniques of final wall contours. They found that the average mass loss was lower than the baseline.

Fixed edge overflow testing is as yet essential for the execution expectation of hub stream blowers and turbines. Zachos et al. [XV]. Finding the general strain misfortune and outlet stream point through the cutting edges is the point of the review. The information will be utilized to approve and adjust a mathematical solver, upgrading its ability to isolate streams. This exploration examines the three-layered direct blower outpouring's presentation at an extremely regrettable frequency point. Comparing a laminar boundary layer to an analogous turbulent layer, Goodhand [XIV] found that the latter has less skin friction. This feature has not yet been applied to the compressor

aerofoil. The leading edge geometry of the aerofoil could be carefully controlled to maintain sizable amounts of laminar flow over its suction surfaces.

Adeniyi et al. [I] used the k - SST cuteness model and the Enormous Swirl Reenactment with the help of ANSYS-CFX to concentrate on the wakes in the field of the stream of a direct flow cut end. This results in pressure differences in the flow of liquid due to the opening between the wall of the end and the tip of the knife. A large speed deficit was found to characterize both the edge wake and the tip leakage vortex. Singoria and Samsher [XX] examined the impact of the sharp edge surface hardness on the optional misfortune of the stream (end loss) and the misfortune of the profile in an air overflow with four reaction cutting edges. These results show that when a 1,000 m roughness is added to both the pressure surface and the suction surface, the mass loss is almost doubled.

The secondary loss is lowest in a cascade with smooth blade suction surfaces and largest in one with rough pressure surfaces. When both surfaces of a blade are rough, the impact of roughness on secondary loss is intermediate.

Azim et al. [XVI] used CFD analysis to study the boundary layer delay in NACA aerofoil on the suction side. At increasing angles of attack, transition flow over airfoils exhibits a great deal of flow instability, including turbulence, boundary layer transition, and localized separation areas. Experiments were performed on the NACA aerofoil cascade of compressor with inlet flow by Zhang et al. [XXII]. The progress zone extends from the pulling surface to the end wall as the unfavorable tension inclination increments, and the way of behaving of the end-wall limit layer decays with expanding entry compressing capacity.

Peyvan and Benisi [V] examined the design of a single-stage axial compressor and forecasted its performance outside the design with a 1D and 3D model. In a single-layer model, conditions are dealt with in the mean line at three main stations: the state output, the rotor bay, and the rotor output. Bai et al. [XVIII] studied the impact of surface hardness on the improvement of limits and misfortunes at the turbine edge with different Reynolds numbers. The result shows that the limit layer speed profile is a smooth edge with a bumpier surface than a smooth edge.

Tang et al. [XXI] studied the robustness effect on the development of 3D corner partitions in a rapid and low-perspective blower cascade. When the two end-side disconnection zones and the first-line dissection point push simultaneously in front of the throat position of the cutting surface, the newly proposed sharp edge attraction surface slows down. Sillitoe et al. [II] used a large-eddy simulation to analyze the border layer transition mechanism of two rectilinear compressor cascades. The study looks at how well different sub-grid scale models work and how unstable wakes affect transition. To create novel compressor designs, it is crucial to accurately forecast the transitional behavior in gas-turbine compressors, as this behavior can have a substantial impact on the compressor's aerodynamic performance.

Baumgartner et al. [VI] explored the impact of the obscure isentropic example on the stream field inside a turbine vane. The researchers led a few exploratory and computational tests that empowered annular fountain testing with different working

liquids and working circumstances, utilizing a newly changed transient air stream. The discoveries show that over the range of isentropic examples assessed, the misfortune could shift by 20% to 35% relying upon the vane leave Mach number. The exploration of the effect of essential mathematical factors and stream qualities on optional stream misfortunes in a turbine overflow was finished by Mesbah et al. [XIII], who distributed the consequences of their mathematical reproduction. The effects of the number of exits of Mach, the pitch-to-chord ratio, the angle of intake, and the angle ratio of the blade on the loss of the end wall and the generation of secondary flow were investigated.

Li et al. [IX] fostered a slowdown expectation model in light of Koch's two-layered diffuser relationship way to deal with evaluate the pivotal stream blower stage's greatest static tension ascent capacity. Dissimilar to the first Koch's model, which just records for the expansion in the channel dynamic strain factor brought about by a high stun point, this paper considers the impact of stream points on the dispersion length and determines the numerical articulation of the changed non-layered dissemination length. Majcher et al. [XII] offer a mathematical process of wind current lift coefficients, drag coefficients, and flux rotation points as part of a cutting-edge overflow configuration approach in a pivotal flow machine. Alongside a procedure and results segment, the paper has an exhaustive classification and catchphrases segment.

The flow of the axial turbine is very complex, 3D, and unstable, resulting in high losses, low efficiency, and low performance. Despite great progress in this field over the past 50 years, the mechanisms for the final flow of the walls are still not very clear. Even today, these flows are a challenging task for turbine designers and researchers. A better understanding of complex three-dimensional flows, their origins, and associated losses will certainly be useful in any attempt to improve turbine performance. Previous work in this field has focused on the two-dimensional geometry of blade profile modeling and simulation. Consequently, the present work is a step forward in comparison with the previous work, and we are trying to see if FLUENT 6.2 can capture complex three-dimensional secondary flow vortices near the end wall area.

The main objective of this study is to perform computational studies on the end-loss phenomena in the turbine steam routes. The analysis includes a three-dimensional computational investigation of the end-loss phenomena of the impulsive blade profile (profile 3525) in a stable turbine flow path. Gambit 2.4.6 is used as a preprocessor [IV], developed a three-dimensional cascade geometry model, and FLUENT 6.2 [VI] is used as a solution and postprocessor for flow simulation. Once the model is verified, more simulations will be performed to investigate the effect of final loss on flow rates of higher Mach values of 0.4 to 0.95, typical of modern utility steam turbines. Simulation results will investigate the impact of roughness on the average mass loss coefficient. It also studied the effects of roughness on secondary losses.

II. Analysis

The friction loss and the secondary loss occur when the liquid flows through the passage of the turbine blade. The roughness of the aerofoil surface has a great influence on these losses. In the current computational study, computational fluid

dynamics (CFD) determined the final loss of a 3D circular wheel turbine cascade by Samsher [XVII].

a) Description of 3D geometry modeling and computational methodology

The accuracy of the computational model depends on the accurate selection of the boundary conditions and the analysis hypotheses. The quality of networks, density, and real geometry representations are the second factors determining computer simulation accuracy. The quality of the grid depends on the shape, low aspect ratio, and low extension ratio of the mesh cell. If further improvements to the network do not change the result, i.e. if grid-dependent solutions are achieved, the grid density is sufficient. The accurate representation of geometry is important, as computer simulation only predicts the flow of ideal models. The accuracy of discrete planning and turbulent modeling is usually dependent on the code and cannot be influenced by the user and it is found by Singoria and Samsher [XX].

The current CFD simulation of the turbine cascade is performed with the commercially available FLUENT 6.2 CFD package as a solution and postprocessor. It is a finite-volume solution based on pressure correction. FLUENT 6.2 is particularly applicable to three-dimensional boundary flow, as the code allows adaptive grids based on gradients to achieve grid-dependent results.

b) Gambit to generate geometry

In CFD analysis, the most important part is the generation of geometry and engraving, which has a major impact on the solution. Therefore, great care should be taken to choose the right sizes of mesh and mesh Singoria and Samsher [XX]. The measurements of the cascade parameters and the flow rate for the test area are shown in Table 1. Gambit 2.4.6 is a preprocessor for the generation of geometry and meshes. First, using the blade profile x and y coordinates to create a two-dimensional model, Gambit 2.4.6 maintained the same dimensions from the input measurement plane to the exit of the tunnel as in the experimental configuration. Then, the 2D model is converted to 3D by dividing the edges of the 2D model by the height of the blade. The flow domains are modeled using four blades instead of six blades in experiments to optimize the power/processor capacity of computers. It is assumed that the flow is symmetric at a medium-range level. The 3D computing domain of the cascade of 3525 turbine blades is shown in Fig. 1.

Table 1: Dimensions of Cascade and other parameters, Samsher [XVII]

Parameters	**Blade-Profile 3525**
Cascade-type	Rectilinear
Inlet cross-section	95 x 93.2 mm^2
Type of test-blade	Impulse type
Blade chord (mm)	50
Blade rows pitch (mm)	29 mm
Blade height (mm)	95

Blade angle	80°
Inlet-angle	40°
Blade numbers	4
Channels numbers	3
Working-fluid	Air
Air inlet temperature	30°C
Velocity at the inlet plane	102m/s
Nature of flow inside cascade	Subsonic (compressible)
Reynolds number at exit	4.7×10^5

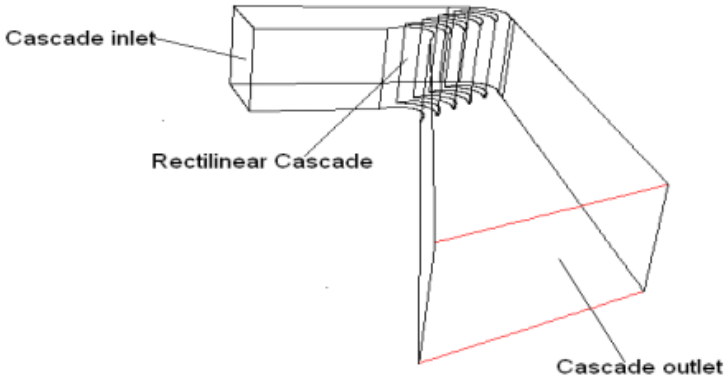

Fig. 1. 3-D computational domain of turbine blade 3525 cascade.

3-D computational domain along with turbine blade 3525 cascade created in Gambit 2.4.6 is shown in Fig. 2.

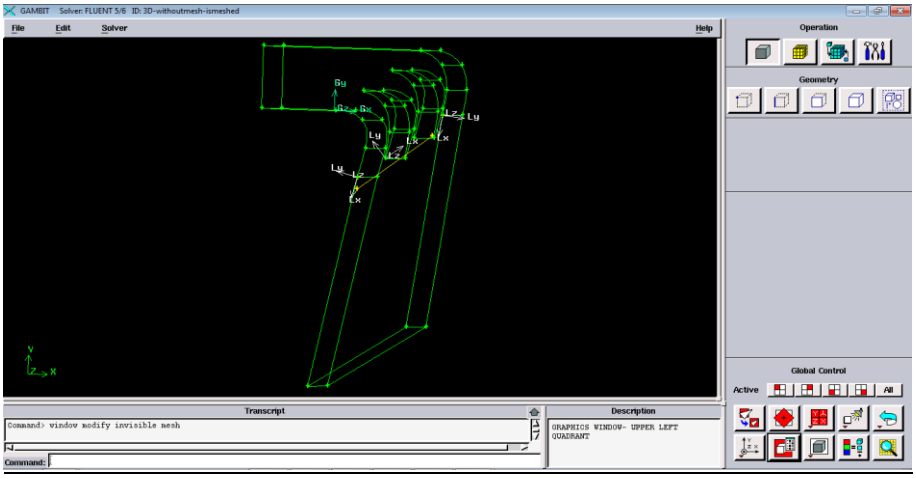

Fig. 2. 3-D computational domain along with turbine blade 3525 cascade

Table 2: Boundary conditions created as zones from various faces & boundary types

Boundary-zone	Inlet-faces	Outlet-faces	External-faces	Suction surfaces 1 to 5	Pressure-surfaces 1 to 5	Bottom end wall	Top end wall
Boundary-type	Velocity-inlet	Pressure-outlet	Wall	Wall	Wall	Wall	Wall

c) Grid generation & Meshing

The mixing of turbomachinery liquid areas involves the mixing of blades and blade passages. Meshes are largely divided into two types, namely structured and non-structured. Consequently, the structured mesh is easy to handle in terms of discretization, linearization, and solution, and is used in current cascade geometry. The typical structure of the blade's blade includes H-line, O-line, and C-line combinations. Each has its advantages and limitations. In general, in Turbomachine laser simulation, structured networks, particularly boundary layers, are preferred and more accurate than non-structured networks. The accuracy of the solution, the cost of computer hardware, and the calculation time needed depend on the quality of the grid. The quality of a good solution network depends on the density of the network, the relationship between the length and volume of adjacent cells, and the tilt. Therefore, every effort is being made to produce a good quality network without excessively increasing the computation cells. The calculation area is shown in Fig. 3.

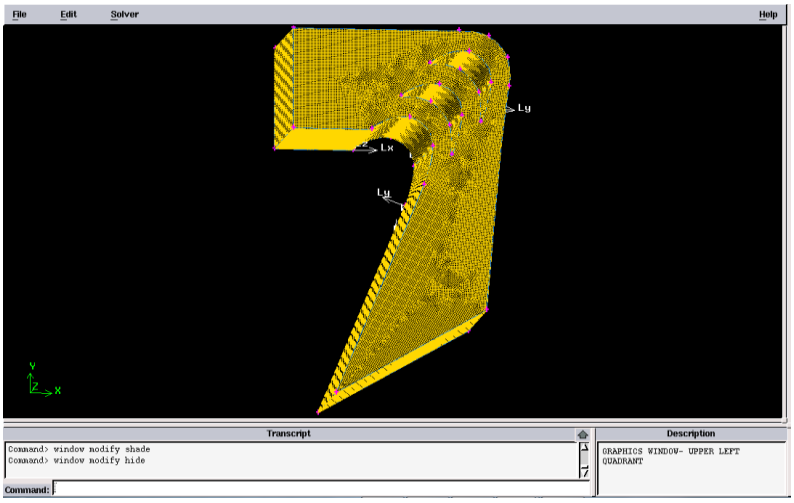

Fig. 3. Meshing of the computational domain

The surface of the 2D geometry profile is swept to generate the volume. The blade pressure and suction surfaces are divided into three parts. This was done to study the effects of localized roughness on secondary loss. The blade volume is removed from the outer shell volume, and the blade position is empty (due to lack of flow). Finally,

the size of the mesh is selected according to the computer capacity of the masked geometry. The areas are as follows. – Pressure input, velocity output, wall, pressure surface, suction surface, wall are also defined. As shown in Table 2 [XX], the boundary conditions created as different faces and boundary types are given names.

d) Validation of results

The present CFD results for the smooth blades were validated with the experimental result obtained by Samsher [XVII] to ensure that the k-epsilon model-RNG which was used in Fluent for simulation purposes is correct as presented in Fig. 4.

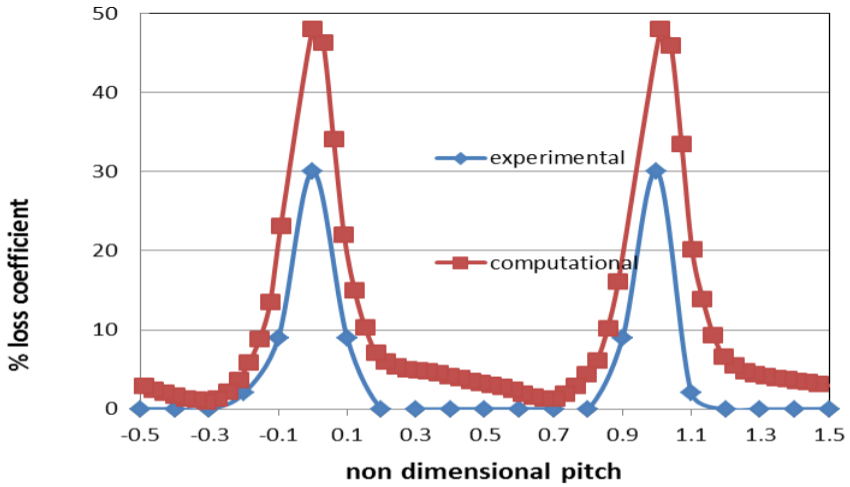

Fig. 4. Computational results validation with that of experimental results by Samsher [XVII]

The results were validated as both graphs appeared to be very close and the % loss coefficient was computed and found to be 6.03%. Two peaks were obtained because only one channel through the cascade was considered. The peaks indicate the presence of both profile-loss and secondary-loss; whereas in the middle portion, the profile of the blade offers no obstruction, and therefore only secondary losses are observed.

III. Results and Discussion

The generated mesh is exported to FLUENT 6.2. The equations of continuous, energy, and momentum are solved separately. A separate solver is used to solve the moment equation for the first time using the guess pressure and generate the pressure correction equation. Due to the "guess and correction" nature of linear systems, many repetitions are usually required. This requires a careful selection of the relaxation parameters of the variables.

After the completion of the model, the quality of the mesh was checked in FLUENT 6.2. The simulation was carried out by a three-dimension double-precision method. As the first step, losses were computed for roughness provided on all surfaces. The total losses for roughness heights of 250, 500, 750, and 1000 micrometers were compared with that for the smooth profile applied separately on all blades: (i) all-pressure-

surfaces (PSR) (ii) all-suction-surfaces (SSR) (iii) both-surfaces (resistance & pressure) of all blades (ASR).

The roughness effects on the suction surface are presented in Fig. 5. Different grades of the roughness of 250µm, 500µm,750µm, and 1000µm were applied and results were obtained. The total blade loss was found to increase with the increase in roughness. The increased losses due to roughness may be attributed to the increased turbulence and earlier boundary layer separation resulting in a wider wake.

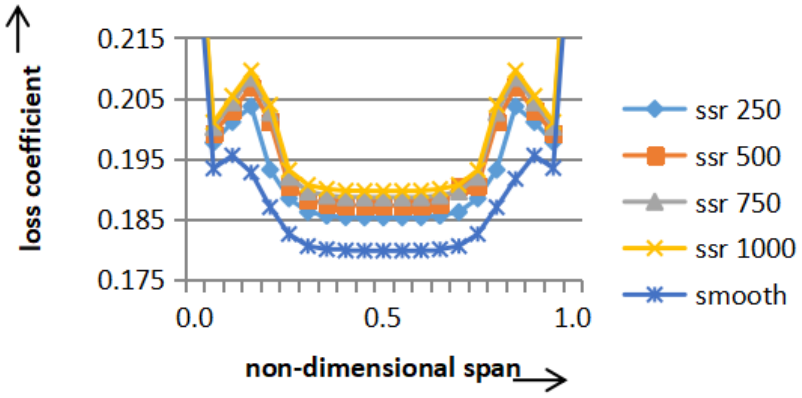

Fig. 5. The variation in total loss along the span with the roughness of the different levels at the suction surface.

The roughness effects when applied to the pressure surface are shown in Fig. 6. Different grades of the roughness of 250µm, 500µm, 750µm, and 1000µm were applied and results were obtained. The total losses were found to meagerly increase with increasing roughness. The reason for the meager increase may be attributed to the lesser effect of roughness on boundary layer separation from the pressure surface.

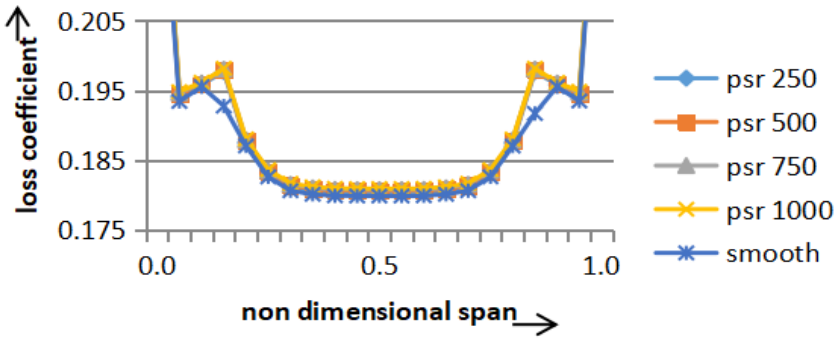

Fig. 6. Variation in total loss along span with roughness of different levels at pressure surface.

The effects of roughness when applied over the entire surface are shown in Fig. 7. Different grades of the roughness of 250µm, 500µm, 750µm, and 1000µm were applied and results were obtained. Here, too the total as well as the profile losses were found to increase with increasing roughness.

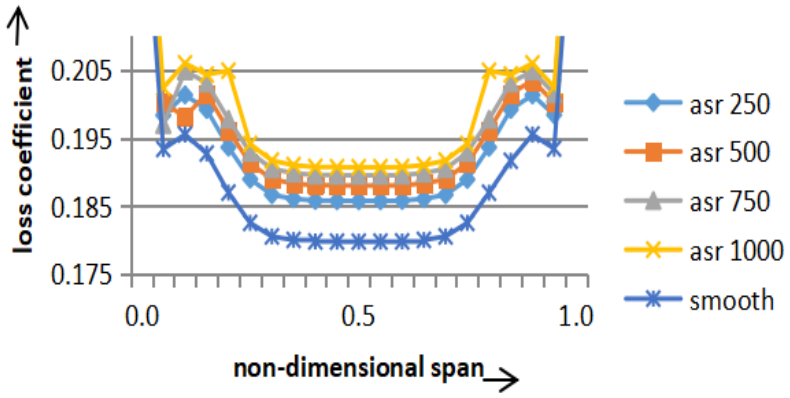

Fig. 7. Variation in total loss along span with the roughness of different levels at the entire surface

The total and profile losses were found to be the maximum in ASR, followed by SSR, followed by PSR, and the lowest in smooth cases, as presented in Fig. 8. The loss of profile in the case of SSR 500 was found to be 3.71% more than that of PSR 500 and 4.13% more in case of ASR 500 for turbine 3525.

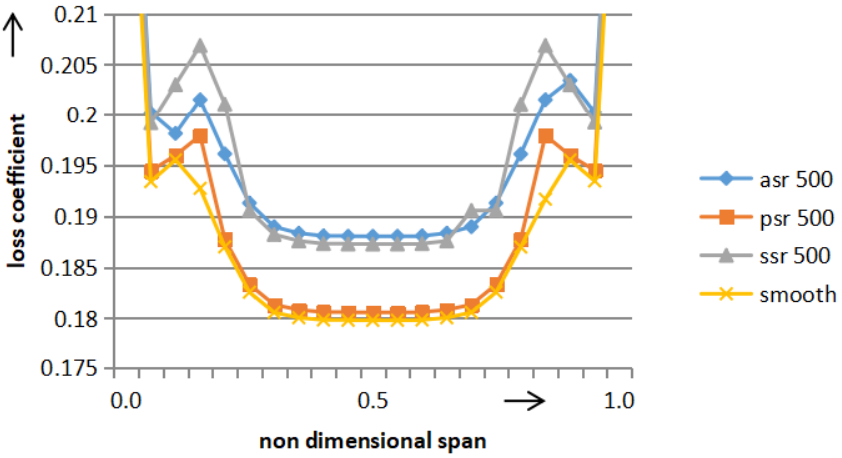

Fig. 8. Variation in total loss along span with roughness of different levels at all surfaces

a) Comparison of secondary losses for turbine profile 3525

The secondary losses or the end losses however show a different trend. In the case of ASR, the end losses initially(250µm) were found to be lower than that of a smooth profile and were found to decrease with increasing roughness up to a grade of 500µm, after which they start showing an increasing trend with increasing roughness. Variation in secondary loss (expressed as % of total loss) for different levels and locations of roughness is shown in Fig. 9. The end losses in the case of PSR were found to be always invariable and almost equal at all roughness grades. The end losses were however found to be greater than that of a smooth profile. The secondary losses in case of SSR was

initially found to increase with increasing roughness up to a roughness grade of 500µm, after which it started showing a decreasing trend.

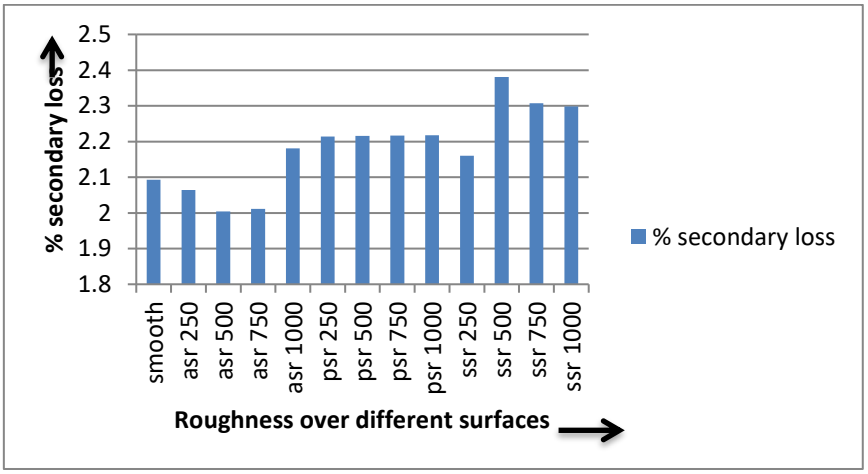

Fig. 9. Variation in secondary loss (expressed as % of total loss) for different levels and locations of roughness

b) Practical Implications

Corrosion is essentially the loss of a turbine material due to a variety of materials that contain contaminants such as steam, water, or gas injection. Erosion is a loss of material due to hard particles present in the stream. The degradation and failure of the turbine components depend on various parameters, such as the Mach number, Reynolds number, the size of the particles, and the material of the particles. Particles with a diameter of less than 10 microns are toxic because they do not have sufficient motion energy to cause erosion. These particles are usually attached to the surface of the blade and accumulate, and the particle diameter exceeds 10 microns, which is less stick efficiency. In essence, erosion is caused by solid particles of large diameter, and the likelihood of erosion is found mainly at the top and bottom of the blade. Despite progress in gas filtration systems, other problems include the formation of particles during combustion by low-grade fuels. Thus, we must analyze the flow behavior of the turbine under the injection of solid and liquid particles.

Using Fluent, you can analyze the length of the blade because, during the flow of fluid, heavy and large-diameter particles hit most of the edge of the blade's release surface, other particles hit the pressure surface of the blade, and almost all of the blades are generated by particles, as you can see in the blade. The shape of the blade is also damaged by the particles as its front and rear edges are completely affected. Lighter particles do not cause erosion but stick to the blade and cause corrosion on the blade. We can eliminate the damage effects by cleaning and polishing the blade, or we can say that some damage losses can be recovered, but erosion losses cannot be recovered. These losses reduce the strength of the blade and the overall efficiency of the turbine. The particle traces describe the path of the particle by the time of the particle's residence, and here we see that, with the increase in diameter, the particle reaches the

top edge, then parallels the length of the blade, and the effect increases in the direction of the suction surface. It can be said that under low speeds and minimal diameter particles, the probability of deposits is higher due to decreased inertia effects. It is recommended to increase the length of the blade by increasing the velocity and diameter of the injection particles on the side of the suction and pressure.

IV. Conclusions

For steam turbines, efficiency is arguably the most crucial performance factor. We can gain a better understanding of the loss mechanisms in steam turbines by researching the impact of end-loss phenomena on machine efficiency. Computer fluid dynamics is used to computerize the end loss phenomena of turbine steam paths. In this study, end-loss phenomena of the Impulse Blade Profile (profile 3525) in the turbine flow path under stable conditions are investigated using three-dimensional computing methods.

Gambit 2.4.6 was used as a preprocessor, FLUENT 6.2 as a solvent, and a postprocessor for flow simulation, creating a three-dimensional model with cascade geometry. After modeling, simulations are performed to examine the impact of end-loss on higher Mach flow in modern commercial steam turbines, with a range of 0.4 to 0.95. Based on simulation results, the impact of roughness on the mass average loss coefficient is investigated. In addition, the impact of roughness on secondary losses is investigated.

It is observed that for a given grade of roughness, the profile losses are found to be maximum for roughness on the suction surface of the mid-chord section and minimum for roughness on the pressure surface of the mid-chord section. The profile loss for roughness being applied on the entire mid-chord section was found to be less. This implies that any roughness on the pressure surface of the mid-chord section tends to reduce total losses. It has also been observed that any roughness applied on the entire leading edge is most detrimental followed by roughness being applied on the entire trailing edge and is least for the mid-chord section. Furthermore, any roughness imparted to a portion of the blade's suction surface is more harmful than the same roughness applied to the blade's pressure surface.

Conflict of Interest

There was no relevant conflict of interest regarding this paper.

References

I. A. A. Adeniyi, A. Mohammed and S. O. Emmanuel. : ‘CFD Modelling of Wakes on Cascade Compressor Blades’. *International Journal of Advances in Science and Technology*. Vol. 4(2), pp. 60-67, 2012.

II. A. D. Scillitoe, P. G. Tucker and P. Adami. : 'Large eddy simulation of boundary layer transition mechanisms in a gas-turbine compressor cascade'. *Journal of Turbomachinery*. Vol. 141(6), pp. 61-68, 2019. 10.1115/1.4042023

III. A. K. Saha and S. Acharya. : 'Computations of turbulent flow and heat transfer through a three-dimensional nonaxisymmetric blade passage'. *ASME Journal of Turbo-machinery*. Vol. 130(3), pp. 1008-1018, 2008. 10.1115/1.2776952

IV. ANSYS Fluent Meshing User's Guide. (2015).

V. A. Peyvan, and A. H. Benisi. : 'Axial-Flow Compressor Performance Prediction in Design and Off-Design Conditions through 1-D and 3-D Modeling and Experimental Study'. *Journal of Applied Fluid Mechanics*. Vol. 9(5), pp. 2149-2160, 2016. 10.18869/acadpub.jafm.68.236.25222

VI. D. Baumgärtner, J. J. Otter and A. P Wheeler. : 'The effect of isentropic exponent on transonic turbine performance'. *Journal of Turbomachinery*. Vol. 142(8), pp. 81-87, 2020. 10.1115/1.4046528

VII. FLUENT, 2005. FLUENT 6.2 Users Guide. Lebanon, USA.

VIII. H. R. Singh and S. R. Kale. : 'A numerical study of the effect of roughness on the turbine blade cascade performance'. *Progress in Computational Fluid Dynamics*. Vol. 8(7), pp. 439-46, 2008. 10.1504/PCFD.2008.021320

IX. J. Li, J. Teng, M. Ferlauto, M. Zhu and X. Qiang. : 'An improved stall prediction model for axial compressor stage based on diffuser analogy'. *Aerospace Science and Technology*. Vol. 127, 2022. 10.1016/j.ast.2022.107692

X. J. Y. Moon and K. S. Yong. : 'Counter-rotating stream-wise vortex formation in the turbine cascade with end wall fencing'. *Int. J. Computers and Fluids*. Vol. 30(4), pp. 473-490, 2001. 10.1016/S0045-7930(00)00026-8

XI. M. J. Brear, H. P. Hodson, P. Gonzalez and N. W. Harvey. : 'Pressure surface separations in low-pressure turbines—Part 2: Interactions with the secondary flow'. *Int. J. Turbomach*. Vol.124(3), pp. 402-409, 2002. 10.1115/1.1450765

XII. M. Majcher, M. Frant and R. Kieszek. : 'Preliminary Numerical Study of a Rectilinear Blade Cascade Flow for a Determination of Aerodynamic Characteristics. *International Review of Aerospace Engineering* (I.RE.AS.E), Vol. 16(4), pp. 143-151, 2023. 10.15866/irease.v16i4.24065

XIII. M. Mesbah., V. G. Gribin and K. Souri. : 'Investigation of the effects of main geometric parameters and flow characteristics on secondary flow losses in a turbine cascade'. *Journal of Physics: Conference Series*. Vol. 3, pp. 21-31, 2021. 10.1088/1742-6596/2131/3/032081

XIV. M. N. Goodhand. : 'Laminar flow compressor blades'. *9th Osborne Reynolds Colloquium and Research Student Award*, Department of Aeronautics Imperial College London, 2011.

XV. P. K. Zachos, N. Grech, B. Charnley, V. Pachidis and R. Singh. : 'Experimental and numerical investigation of a compressor cascade at highly negative incidence'. : '*Engineering Applications of Computational Fluid Mechanics*. Vol. 5(1), pp. 26-36, 2011. 10.1080/19942060.2011.11015350

XVI. R. Azim, M. M. Hasan and M. Ali. : 'Numerical investigation on the delay of boundary layer separation by suction for NACA 4412'. *Procedia Engineering*. Vol. 105, pp. 329-334, 2015. 10.1016/j.proeng.2015.05.013

XVII. Samsher. : 'Effects of localized roughness over reaction and impulse blades on loss coefficient'. *Proceedings of the Institution of Mechanical Engineers, Part A: Journal of Power and Energy*. Vol. 221(1), pp. 21-32, 2007. 10.1243/09576509JPE214

XVIII. T. Bai, J. Liu, W. Zhang, and Z. Zou. : 'Effect of surface roughness on the aerodynamic performance of turbine blade cascade'. *Propulsion and Power Research*. Vol. 3(2), pp. 82-89, 2014. 10.1016/j.jppr.2014.05.001

XIX. T. Sonoda, M. Hasenjäger, T. Arima and B. Sendhoff. : 'Effect of end wall contouring on performance of ultra-low aspect ratio transonic turbine inlet guide vanes'. *ASME Journal of Turbomachinery*. Vol. 131(1), pp. 11020-11031, 2009. 10.1115/1.2813015

XX. V. K. Singoria and Samsher. : 'The Study of End Losses in a Three Dimensional Rectilinear Turbine Cascade'. *Int. J. of Emerging Technology and Advanced Engineering*. Vol. 3(8), pp. 782-797, 2013. https://www.scribd.com/document/389319869/IJETAE-0813-122

XXI. Y. Tang, Y. Liu and L. Lu. : 'Solidity effect on corner separation and its control in a high-speed low aspect ratio compressor cascade'. *Int. J. of Mechanical Sciences*. Vol. 142, pp. 304-325, 2018. 10.1016/j.ijmecsci.2018.04.048

XXII. Zhang, Y. Wu, Y. Li, and H. Lu. : 'Experimental investigation on a high subsonic compressor cascade flow'. *Chinese Journal of Aeronautics*. Vol. 28(4), pp. 1034-1043, 2015. 10.1016/j.cja.2015.06.019